Cyclic Strength of Sand under Sustained Shear Stress

J. Yang, M.ASCE[1]; and H. Y. Sze, A.M.ASCE[2]

Abstract: The existence of initial shear stress can have a significant effect on the cyclic strength or liquefaction potential of sand. This effect is not yet fully understood because of a lack of convergence and consistency in the existing data and interpretations, leading to great uncertainty in quantifying the effect for practical applications. This paper presents new experimental results on a silica sand to validate the concept known as threshold α, below which the cyclic strength of sand increases with α and above which the cyclic strength decreases with α (with α representing the sustained shear stress level). On the basis of a series of monotonic loading tests on the same sand, and in the framework of critical state soil mechanics, it is further confirmed that threshold α can be well related to a state parameter in the void ratio-mean effective stress plane and thereby a unified and consistent interpretation can be established. A new platform is proposed on which the relationship between cyclic strength and state parameter is represented by a linear line, and this line will rotate clockwise as α increases. This platform provides an effective analytical tool for the study of the effect of sustained shear stress on the cyclic strength of sand. Moreover, the study also shows that the cyclic loading path is well linked with the monotonic loading path under different sustained shear stress levels, and this correspondence sheds light on the mechanisms underlying a variety of experimental observations. **DOI: 10.1061/(ASCE)GT.1943-5606.0000541.**

CE Database subject headings: Cyclic strength; Shear stress; Failures; Laboratory tests; Soil liquefaction; Sand (soil type).

Author keywords: Critical state; Cyclic strength; Failure; Laboratory tests; Liquefaction; Sands.

Introduction

The undrained response and strength of sand under cyclic loading is of both practical and theoretical interest. Since the pioneering work of Seed and Lee (1966), a number of fundamental issues on cyclic loading behavior of sand have been addressed through well-controlled laboratory experiments. In particular, extensive studies have been focused on reconstituted sand specimens under two-way, symmetrical loading in compression and extension. This loading condition principally aims to represent the free-field level ground under earthquakes (Seed 1979; Toki et al. 1986). In many practical applications involving earth dams and slopes, however, the elements of soil are subjected to static shear stresses on the horizontal planes before the earthquake loading comes into effect. Such initial, sustained shear stresses also exist in the soil beneath the edges of buildings or structures. To replicate this condition in triaxial tests, a sand specimen needs to be consolidated anisotropically to yield an initial shear stress in it (Seed 1983; Vaid and Chern 1985; Mohamad and Dobry 1986; Hyodo et al. 1994; Vaid et al. 2001); superposition of a cyclic deviatoric stress then produces cyclic loading that is asymmetrical about the hydrostatic stress state. The level of sustained shear stress can be characterized by a parameter α, defined as the ratio between the sustained shear stress and the effective confining stress on the maximum shear stress plane.

Although the importance of sustained shear stress has long been recognized, its effect on cyclic strength has not yet been fully understood. Several experimental studies have suggested that the presence of sustained shear stress enhances the cyclic strength or liquefaction resistance of sand. Several others have, however, indicated the opposite tendency. The compilations and analyses of published data by Seed and Harder (1990) and Harder and Boulanger (1997) show the important density dependence of the effect; that is, the effect is beneficial to liquefaction resistance for dense sand with a relative density of approximately $55 \sim 70\%$ but is detrimental for loose sand with a relative density of approximately 35%. Given the lack of convergence and consistency in the existing data and interpretations, the National Center for Earthquake Engineering Research (NCEER) committee (Youd et al. 2001) did not recommend any proposal for routine engineering practice but underscored the need for continued research on this issue.

With the aim of producing a comprehensive database to help resolve the uncertainty, Yang and Sze (2011) performed an experimental study consisting of more than 120 cyclic triaxial tests on Toyoura sand. These tests covered a broad range of initial states in relative density, confining pressure, and static shear stress level. A threshold α was found to exist below which the cyclic strength of sand increases with increasing α but above which the strength tends to reduce with α. Moreover, the threshold α was found to depend on both relative density and confining stress and can, in line with the critical state concept, be related to a state parameter ψ proposed by Been and Jefferies (1985). Because these findings show an attractive potential in developing a unified and consistent interpretation for the effect of sustained shear stress, further verification through laboratory experiments on different sands is both necessary and desirable. These additional experiments can also offer an enlarged data source that will be useful in the efforts to quantify the effect of sustained shear stress for practical applications (Idriss and Boulanger 2003, 2008).

Against this background, a series of cyclic tests has been conducted on a silica sand called Fujian sand, which is the Chinese

[1]Associate Professor, Dept. of Civil Engineering, Univ. of Hong Kong, Pokfulam Rd., Hong Kong, China (corresponding author). E-mail: junyang@hku.hk

[2]Ph.D. Student, Dept. of Civil Engineering, Univ. of Hong Kong, Pokfulam Rd., Hong Kong, China.

Note. This manuscript was submitted on May 11, 2010; approved on March 16, 2011; published online on March 17, 2011. Discussion period open until May 1, 2012; separate discussions must be submitted for individual papers. This paper is part of the ***Journal of Geotechnical and Geoenvironmental Engineering***, Vol. 137, No. 12, December 1, 2011. ©ASCE, ISSN 1090-0241/2011/12-1275–1285/$25.00.

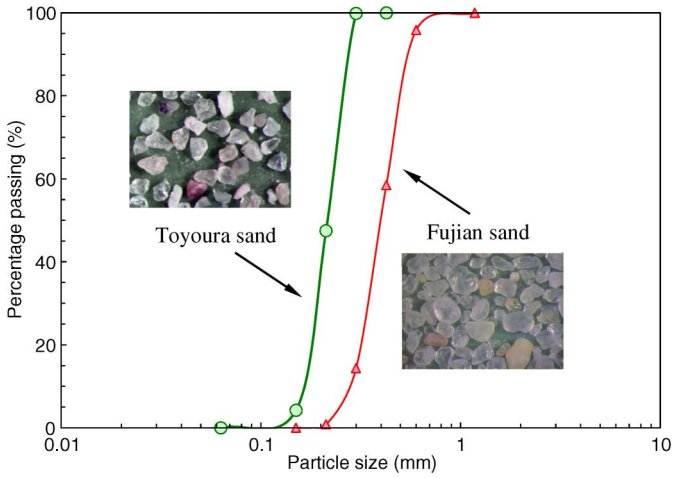

Fig. 1. Particle size distributions of Fujian sand and Toyoura sand

standard sand, to examine whether the concept of threshold α holds as well. A critical state-based analysis of the new data will be presented to check the effectiveness of the use of the state parameter in characterizing the cyclic strength of sand under sustained shear stress. In particular, on the basis of a detailed analysis of the abundant and systematic data sets from Fujian sand and Toyoura sand, a new notion—termed as "α-induced rotation of strength lines"—is developed in the cyclic strength-state parameter plane to characterize the sustained shear effect. A series of monotonic loading tests on Fujian sand has also been performed. Representative results from these monotonic tests will be presented to develop a linkage between the monotonic and cyclic stress paths that, as will be shown later, can help capture in a rational way the mechanisms for a variety of experimental observations.

Material and Test Program

Both Fujian sand and Toyoura sand are uniform silica sands, but the former has coarser and more rounded grains. Fig. 1 compares the particle size distribution curves of the two sands and shows the microscopic views of the two sands. The basic properties of the two sands are summarized in Table 1.

All cyclic triaxial tests on Fujian sand, as listed in Table 2, were performed by using an automated triaxial testing system, which was also used in testing Toyoura sand. Moist tamping with undercompaction consideration was used to prepare sand specimens. Because the cyclic resistance of sand is sensitive to the degree of saturation (Yang et al. 2004), full saturation was conducted carefully for each specimen. Anisotropic consolidation was conducted by controlling the principal consolidation stresses σ'_{1c} and σ'_{3c} in segments such that a constant initial static shear stress ratio was maintained in each segment until the targeted stress condition was reached (Yang and Sze 2011). The sustained shear stress level is characterized by α as

Table 2. Cyclic Triaxial Tests Conducted on Fujian Sand

Initial relative density, D_{rc} (%)	Initial confining pressure, σ'_{nc} (kPa)	Minor principal stress, σ'_{3c} (kPa)	Initial static shear stress ratio, α	Initial static deviatoric stress, q_s (kPa)	Cyclic deviatoric stress, q_{cyc} (kPa)
20	100	100	0	0	35
20	100	100	0	0	40
20	100	100	0	0	45
20	100	90	0.1	20	40
20	100	90	0.1	20	45
20	100	90	0.1	20	50
20	100	75	0.25	50	50
20	100	75	0.25	50	55
20	100	60	0.4	80	45
20	100	60	0.4	80	50
20	100	40	0.6	120	—
50	100	100	0	0	60
50	100	100	0	0	70
50	100	90	0.1	20	60
50	100	90	0.1	20	70
50	100	60	0.4	80	110
50	100	60	0.4	80	120

$$\alpha = \frac{q_s}{2\sigma'_{nc}} = \frac{\sigma'_{1c} - \sigma'_{3c}}{\sigma'_{1c} + \sigma'_{3c}} \quad (1)$$

where q_s = deviatoric stress and σ'_{nc} = effective confining stress on the maximum shear stress plane. After consolidation, cyclic deviatoric stress q_{cyc} was applied on the specimen in undrained conditions. If q_{cyc} exceeds q_s in magnitude, loading is said to be with stress reversal; otherwise, it is without reversal.

In addition to the cyclic tests, a series of monotonic compression and extension tests was conducted on Fujian sand (Table 3). These tests were aimed principally at yielding contractive responses and critical states for developing a better interpretation and understanding of the framework of critical state soil mechanics. The monotonic loading tests covered a range of relative densities ($D_{rc} = 10 \sim 70\%$) under two different confining stress levels ($\sigma'_{nc} = 100$ and 500 kPa) and two sustained shear stress levels ($\alpha = 0$ and 0.4). Selected test results will be presented to assist in the analysis of the cyclic test data.

Cyclic Failure Patterns

On the basis of a large number of systematic tests on Toyoura sand, Yang and Sze (2011) have identified three distinct cyclic failure patterns. They are broadly categorized, depending on the initial state and the stress reversal degree, as flow-type failure, cyclic mobility, and plastic strain accumulation. These failure modes were also typical for Fujian sand, as briefly discussed here.

Fig. 2 presents the cyclic behavior of Fujian sand at loose state ($D_{rc} = 20\%$ and $\sigma'_{nc} = 100$ kPa). Regardless of whether a sustained shear stress was present, flow-type failure or abrupt runaway

Table 1. Physical Properties of Fujian Sand and Toyoura Sand

Sand	Mean grain size (D_{50}, mm)	Coefficient of uniformity (C_u)	Coefficient of curvature (C_c)	Specific gravity (G_s)	Maximum void ratio (e_{max})	Minimum void ratio (e_{min})
Toyoura	0.216	1.392	0.961	2.64	0.977	0.605
Fujian	0.397	1.532	0.971	2.65	0.879	0.555

Table 3. Monotonic Loading Tests Conducted on Fujian Sand

Loading mode	Initial relative density, D_{rc} (%)	Initial confining pressure, σ'_{nc} (kPa)	Minor principal stress, σ'_{3c} (kPa)	Initial static shear stress ratio, α	Initial static deviatoric stress, q_s (kPa)
Compression	10	100	100	0	0
	10	100	60	0.4	80
	10	500	500	0	0
	15	500	500	0	0
	20	100	100	0	0
	20	100	60	0.4	80
	20	500	500	0	0
	20	500	300	0.4	400
	30	100	100	0	0
	30	500	500	0	0
	35	100	100	0	0
	35	100	60	0.4	80
	35	500	500	0	0
	50	100	100	0	0
	50	100	60	0.4	80
	50	500	500	0	0
	50	500	300	0.4	400
	70	100	100	0	0
	70	100	60	0.4	80
Extension	10	100	100	0	0
	20	100	100	0	0
	35	100	100	0	0

deformation was found to be the unique pattern. The presence of sustained shear stress and the degree of stress reversal only dictated the direction of excessive deformation. The excess pore water pressure (PWP) underwent a sudden and dramatic rise at some point in the course of loading, accompanied by rapid and abrupt straining; before that point, the pore pressure showed a gradual buildup associated with unnoticeable deformation. This flow-type failure, if occurring in situ, may cause catastrophic consequences because of its sudden nature.

Fig. 3 illustrates the response of Fujian sand at medium dense state ($D_{rc} = 50\%$ and $\sigma'_{nc} = 100$ kPa) under asymmetrical loading (i.e., $\alpha > 0$). The failure patterns differ in regard to the degree of stress reversal. As shown in Fig. 3(a), cyclic mobility prevailed even at a very high sustained shear stress level ($\alpha = 0.4$), as long as there was sufficient stress reversal. Although the initial pore pressure and deformation mechanisms remained similar to that of loose sand, the flow-type failure did not occur. At the time when the pore pressure was close to the initial confining stress level, that is, the so-called state of initial liquefaction (Ishihara 1996), the increase in axial strain became substantial. Because the attainment of zero effective stress was temporary, the associated softening was transient and did not cause collapse. Instead, as loading proceeded, the sample regained its strength and stiffness as a result of dilation. This loop repeated itself in subsequent cycles, accompanied by a steady-state response of pore pressure, but the sample kept deforming with a strain accumulation up to 20% in double amplitude. Such excessive deformations, if occurring at the site, may bring about severe serviceability problems. The presence of sustained shear in this case resulted in soil deformations more biased in compression.

If the sustained shear stress became larger in magnitude than the cyclic deviatoric stress such that no stress reversal took place, the mode of plastic strain accumulation would take place, as shown in Fig. 3(b). Pronounced deformation was accumulating in a single direction during the entire loading process, whereas the pore pressure was not built up to a high level. This observation implies that in this failure mode the accumulation of irreversible strains is more critical than the buildup of pore pressure. The specimen shown in Fig. 3(b) was consolidated at a relative density of 35% and a confining stress level of 100 kPa. A common practice would be to treat it as a "loose" sand sample; however, it exhibited a behavioral response differing from that of truly loose samples shown in Fig. 2 in several key aspects, including the generation of pore pressure and the evolution of axial strain and stress path, and it did not fail in the abrupt flow manner. As will be shown later, in the framework of critical state soil mechanics, this sample was actually at a dense state, meaning that it should have potential for a dilative response. This observation underlines the rationale and importance of a critical state-based analysis of cyclic test data.

Cyclic Shear Resistance

Yang and Sze (2011) proposed a consistent way to define failure in characterizing cyclic shear resistance, which is apparently applicable to Fujian sand in this study. In short, the onset of flow failure is defined uniquely for loose sand as the triggering of sudden runaway deformation (Fig. 2); for medium dense sand, it is defined as the attainment of 5% double-amplitude axial strain in the case of cyclic mobility [Fig. 3(a)]; and in the case of plastic strain accumulation, it is defined as the attainment of 5% peak axial strain [Fig. 3(b)]. Given these failure criteria, the number of loading cycles at failure can be picked out for each test and a cyclic stress ratio CSR_n is determined as

$$CSR_n = \frac{q_{cyc}}{2\sigma'_{nc}} \tag{2}$$

where n = use of σ'_{nc} as the denominator, which is in contrast to the conventional use of σ'_{3c}. This choice is considered more reasonable because it is σ'_{nc} that replicates the in situ overburden pressure. Cyclic shear strength is then defined as the value of CSR_n at 10 cycles of loading and denoted as CRR_n (cyclic resistance ratio) for further analysis. The choice of 10 cycles is consistent with the recommendation by Ishihara (1996).

Effect of Relative Density

Fig. 4(a) shows the variation of CRR_n values of Fujian sand with relative density (D_{rc}) for different α levels at the confining stress $\sigma'_{nc} = 100$ kPa. Evidently, the denser the sand, the greater the cyclic shear strength. More importantly, it is found that this trend is largely dependent on the sustained shear stress level. If no sustained shear stress is present or the sustained shear stress is at a low level ($\alpha = 0.1$), the rate of change in strength between loose and medium dense state is almost the same. However, when the sustained shear stress is present at a high level ($\alpha = 0.4$), the rate of change in strength increases dramatically.

In Fig. 4(b), the data points of Fujian sand are superimposed to that of Toyoura sand for the purpose of comparison. A remarked feature is that Fujian sand and Toyoura sand tend to share almost the same CRR_n values if their initial states in relative density, confining stress, and static shear stress are the same.

Effect of Sustained Shear Stress

The variation of the cyclic strength of Fujian sand with α is shown together with that of Toyoura sand in Fig. 5(a). Again, the CRR_n values of the two sands are quite close and show a consistent trend. For samples at medium dense state ($D_{rc} = 50\%$), the presence of

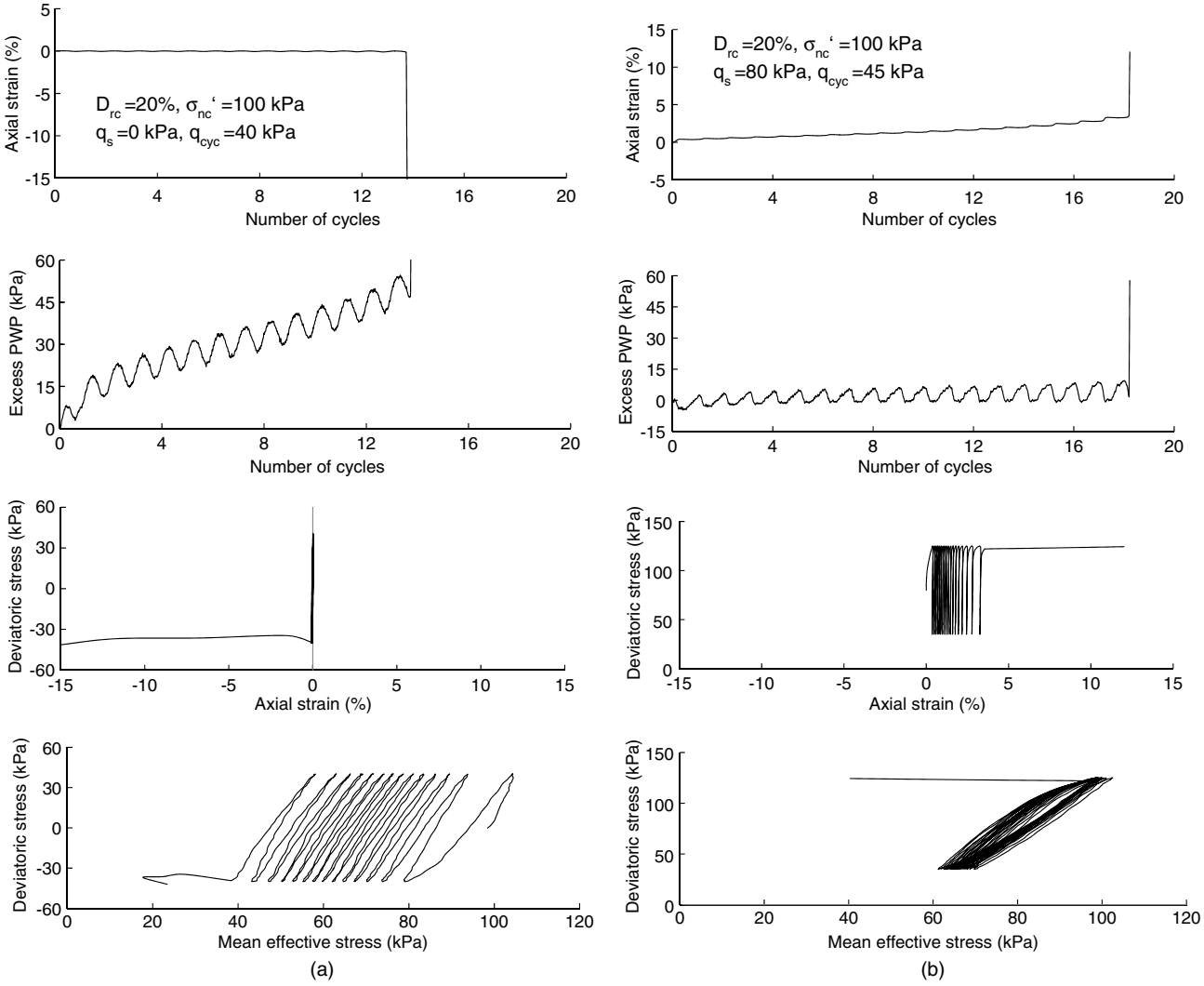

Fig. 2. Cyclic response of loose Fujian sand under (a) $\alpha = 0$; (b) $\alpha = 0.4$

sustained shear stress up to $\alpha = 0.4$ always enhances cyclic strength. For samples at loose state ($D_{rc} = 20\%$), the effect is not straightforward—the cyclic strength or liquefaction resistance first increases and then decreases with α. Obviously, the concept of threshold α and the no-stress-reversal line proposed by Yang and Sze (2011) apply to Fujian sand as well. The threshold α, above which the CRR_n tends to decrease, is approximately 0.25 for Fujian sand at $D_{rc} = 20\%$. This value can be well predicted by the intersection between the $CRR_n - \alpha$ curve and the no-stress-reversal line. Here, the no-reversal line acts as the boundary between loading zones with and without stress reversal. For both sands at $D_{rc} = 50\%$, because the $CRR_n - \alpha$ curves have not yet reached the no-stress-reversal line, the strength reduction does not occur.

The loose sand samples tend to undergo significant reduction in strength beyond the threshold α level, all the way down to $CRR_n = 0$ at $\alpha = 0.6$; at $\alpha > 0.4$, the cyclic strength drops below the values corresponding to the case of zero sustained shear stress ($\alpha = 0$). This observation suggests that caution should be exerted whenever large sustained shear stresses are probably present, because substantial destabilization may be triggered by such an amount of initial shear.

To characterize the effect of sustained shear stress, the K_α correction factor, first proposed by Seed (1983), is introduced here as the ratio of CRR_n at any α to that at $\alpha = 0$ under a fixed σ'_{nc}. The K_α versus α relation for Fujian sand is compared with that of Toyoura sand in Fig. 5(b). Obviously K_α values vary with α in the same manner as that of CRR_n values, leading to a similar and close $K_\alpha - \alpha$ trend of the two sands.

Effect of Sand Types

The foregoing detailed comparisons of Fujian sand and Toyoura sand, in regard to cyclic response and shear strength under various initial states, are necessary and important. Apart from demonstrating that the laboratory tests are highly repeatable and reliable, they confirm the concept of threshold α and the effectiveness of the use of the no-stress-reversal line. They also suggest that the differences in particle size and particle angularity for the two sands, which are not very significant, have a minor effect on their response and strength. Because both sands have similar coefficients of uniformity and curvature (see Fig. 1 and Table 1), it is speculated that the uniformity of sand might play a more controlling role.

Critical State-Based Analysis

The use of the critical state concept to interpret cyclic strength and threshold α has been shown to be effective and attractive for Toyoura sand (Yang and Sze 2011). The central point of critical state soil mechanics (Schofield and Wroth 1968) is that an ultimate state of shear failure exists at which the sand deforms continuously

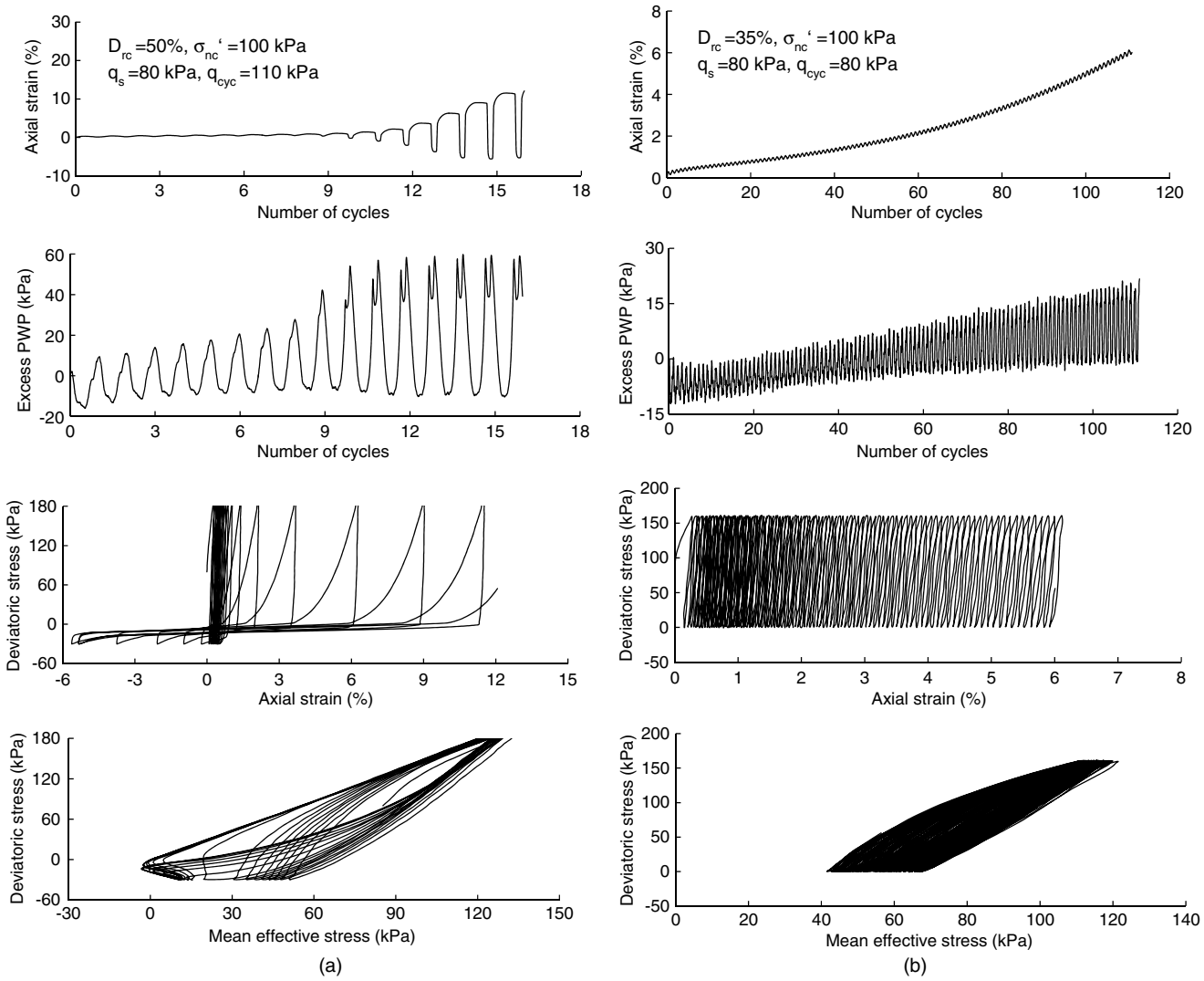

Fig. 3. Cyclic response of medium dense Fujian sand under $\alpha = 0.4$ with (a) partial stress reversal; (b) zero stress reversal

under constant stress and constant volume and the locus of the critical states in the $e - \log p'$ plane constitutes the critical state line (CSL). Here p' is the mean effective stress. To derive the critical state line of Fujian sand, a series of undrained monotonic compression tests was performed. Fig. 6 shows results of two representative samples: one was sheared at very loose state ($D_{rc} = 9\%$ and $\sigma'_{3c} =$ 100 kPa), showing a significant contractive response, and the other was sheared at medium dense state ($D_{rc} = 50\%$ and $\sigma'_{3c} = 100$ kPa) with a dilative response. The determined critical state line of Fujian sand is shown in Fig. 7, together with that of Toyoura sand determined by Verdugo and Ishihara (1996), both showing a reasonably similar trend in the $e - \log p'$ plane. For further analysis, the critical state line of Fujian sand is approximated here by using the power law

$$e_{cs} = 0.8374 - 0.0227\left(\frac{p'_{cs}}{p'_a}\right)^{0.7} \tag{3}$$

where e_{cs} and p'_{cs} = void ratio and mean effective stress at the critical state, respectively, and p'_a = atmospheric pressure.

Cyclic Strength and State Parameter

The state parameter ψ of Been and Jefferies (1985) is a useful index to account for the initial state of sand in regard to relative density and confining stress in liquefaction analysis (Yang 2002; Boulanger 2003; Jefferies and Been 2006). It is defined as the difference between the initial void ratio e_0 of sand and its void ratio at critical state e_{cs} at the same mean stress such that $\psi = e_0 - e_{cs}$(see Fig. 7). At a given initial state, the contractiveness or dilativeness of sand is represented by the value of ψ; a positive ψ value means that the sand is at a loose, contractive state, whereas a negative ψ value implies that it is at a dense, dilative state.

Fig. 8(a) shows the determined CRR_n values against state parameter for Fujian sand and Toyoura sand mixed for various α levels. A fairly good correlation exists between CRR_n and ψ, showing that cyclic strength decreases with increasing ψ or as sand becomes more contractive. The straight line plotted in the figure is a linear representation proposed by Yang and Sze (2011) for test data of Toyoura sand:

$$CRR_n = -2.2376\psi + 0.1837 \tag{4}$$

The data points of Fujian sand appear to fit the trend well, indicating that the effectiveness of the use of ψ in the interpretation of cyclic strength is not affected by the differences in physical properties of the two sands. This is considered reasonable because the critical state line should have already reflected physical properties that are attributed to a particular sand type.

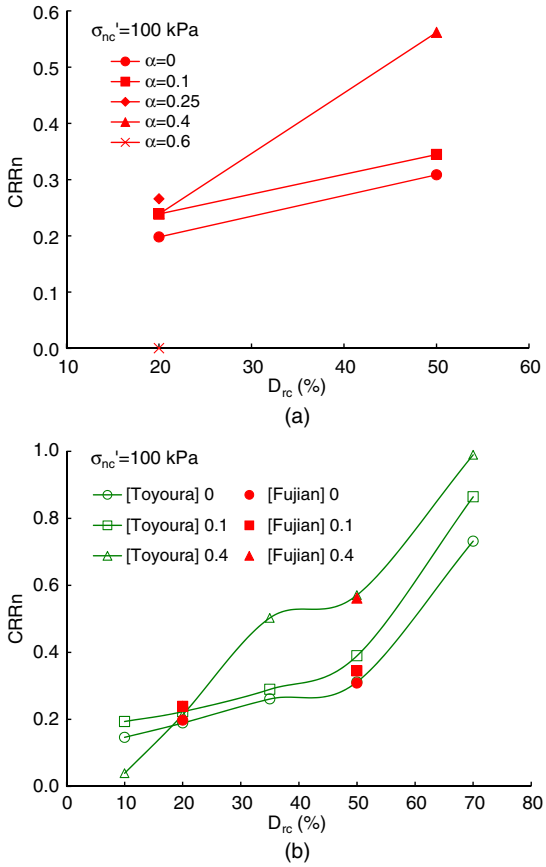

Fig. 4. Effect of relative density on cyclic strength under various α values: (a) Fujian sand; (b) Fujian sand versus Toyoura sand

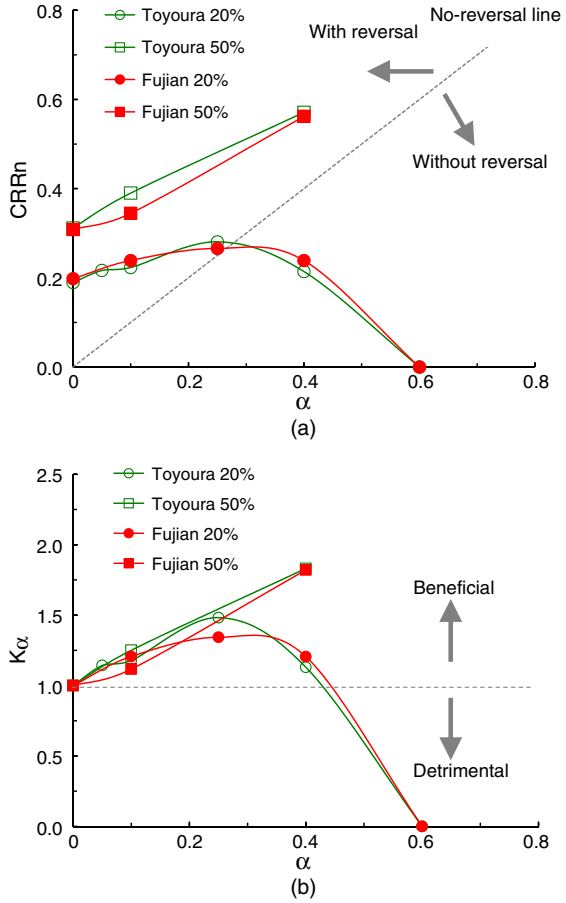

Fig. 5. Variation of (a) cyclic strength; (b) $K\alpha$ with α

A nonlinear correlation between CRR_n and ψ was also proposed by Yang and Sze (2011) for Toyoura sand, as shown in Fig. 8(b) together with the data points of Fujian sand. This nonlinear relationship is given by

$$\mathrm{CRR}_n = 8.1508\psi^2 - 1.2895\psi + 0.1498 \tag{5}$$

Rotation of $\mathrm{CRR}_n - \psi$ *Lines with* α

Although a fairly good correlation can be established for both sands for the first instance, the data points in Fig. 8 are somehow scattered. To examine this scattering, the $\mathrm{CRR}_n - \psi$ data are replotted in Fig. 9 with proper categorization according to α levels, separately for Toyoura sand and Fujian sand. The scatter is primarily attributable to the presence of sustained shear stress at different levels. At each α, the $\mathrm{CRR}_n - \psi$ trend can be well represented by a linear line as given in the plot. In this way, a set of linear equations can be calibrated for Toyoura sand in Fig. 9(a), relating the cyclic resistance and state parameter for a spectrum of α values. As expected, these equations also work well for Fujian sand [Fig. 9(b)].

When the sand is at a greater sustained shear stress level, it tends to show a larger rate of reduction in strength with the state parameter. In other words, as α increases from zero, the slope of the corresponding $\mathrm{CRR}_n - \psi$ line will keep increasing. Given that the $\mathrm{CRR}_n - \psi$ linearity can always be maintained, varying α from low to high levels simply brings about clockwise rotation of the trend line without a fixed pivot. Despite the availability of fewer data points for Fujian sand, the same observation remains in its case. This new finding, along with the concept of threshold α, is of particular importance in understanding the complicated effect of sustained shear stress, because it allows a unified, consistent, and rational interpretation to be established, as will be elaborated next.

Threshold α *on the* $\mathrm{CRR}_n - \psi$ *Platform*

The α categorization of $\mathrm{CRR}_n - \psi$ lines makes it possible to determine, at any combination of ψ and α, the corresponding magnitude of cyclic strength. This allows the $\mathrm{CRR}_n - \alpha$ path to be tracked at any ψ state by reading the change of CRR_n from the line at $\alpha = 0$ to that at greater α levels. Referring to a simple case of two crossing $\mathrm{CRR}_n - \psi$ lines in Fig. 10(a), CRR_n increases with α at ψ_1 state, but it shows a drop at ψ_2 state. Because of the α-induced rotation, these two lines must be crossing at a certain level of state parameter ψ_{cross}. As long as the current state is more dilative, the increasing trend of CRR_n must be maintained. Otherwise, a strength reduction is anticipated.

When more $\mathrm{CRR}_n - \psi$ lines are available, a more complete $\mathrm{CRR}_n - \alpha$ trend can be extracted. Fig. 10(b) presents an example of three lines, designated as Line 1 ($\alpha = 0$), 2 (low α), and 3 (high α). Following the same notion, at a sufficiently dilative ψ_1 state, the cyclic strength CRR_n increases all the way from Line 1 to Line 3 because ψ_1 is well below any ψ_{cross}—this is exactly the response of sand at medium dense state as shown in Fig. 5. When sand becomes more contractive (e.g., D_{rc} reduces from 50 to 20%), Line 3 exhibits the greatest declination so that it subsequently crosses with Line 2 and then Line 1. At some states such as ψ_2, CRR_n only shows an initial rise from $\alpha = 0$ to low α level because Lines 1 and 2 have not yet crossed. However, a substantial drop in CRR_n will occur when α is brought to a greater level. In this case, the threshold

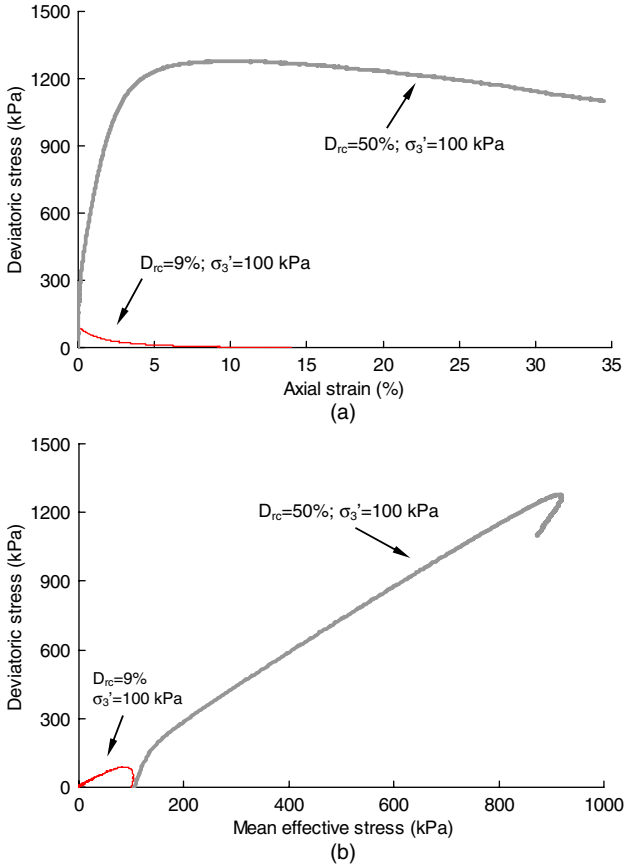

Fig. 6. Representative results of monotonic tests on Fujian sand: (a) stress-strain behavior; (b) stress path

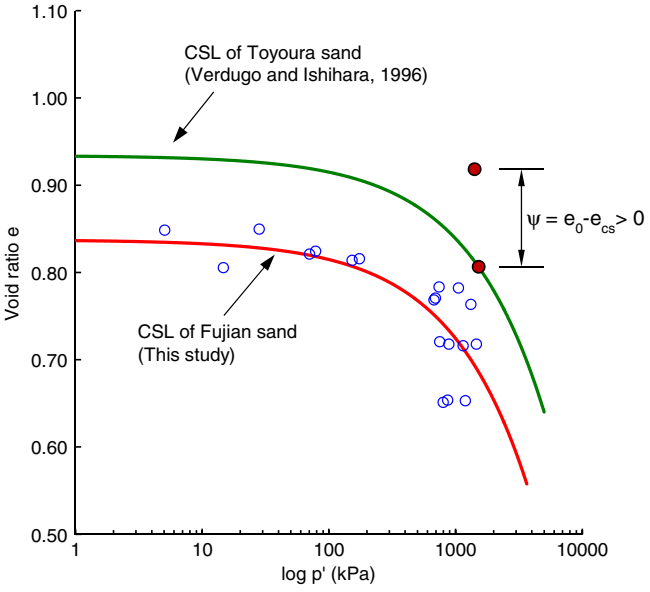

Fig. 7. Critical state lines of Fujian sand and Toyoura sand

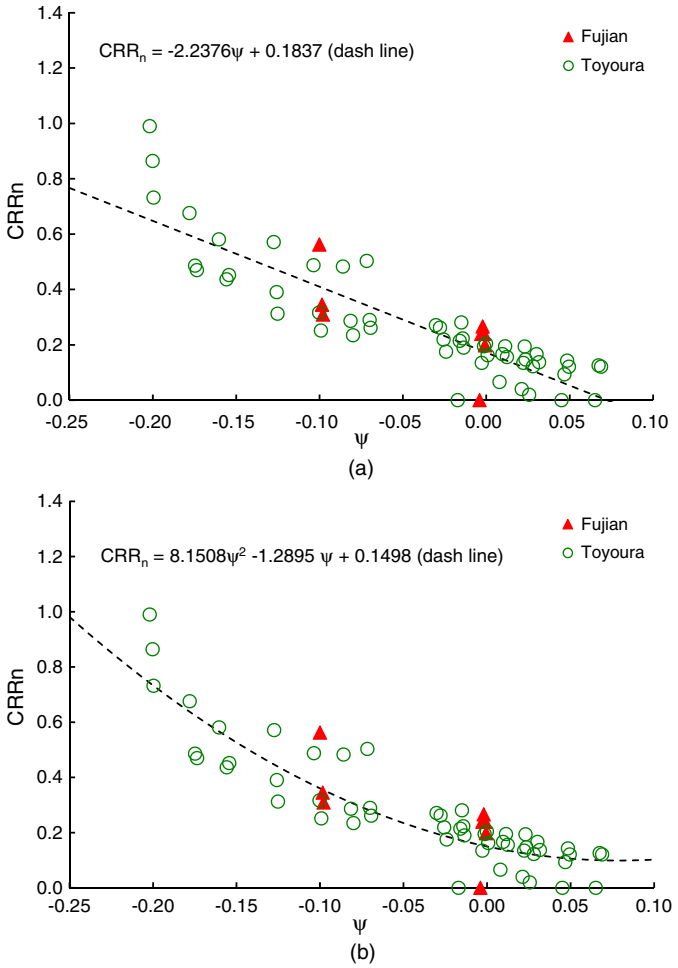

Fig. 8. Correlation between CRR_n and ψ without α value categorization: (a) linear representation; (b) nonlinear representation

α is actually the low α level for ψ_2 state because the value of CRR_n attains its local maximum there.

In general, on the $CRR_n - \psi$ platform proposed here, the threshold α at a certain ψ state is the α level for which the $CRR_n - \psi$ line positions the upmost among others at this ψ. Considering a family of lines under continuous α-induced rotation, different lines would, because of the multiple crossing, take the turn to sit at the upmost position at different ψ states—this follows exactly the concept of the no-stress-reversal line, which suggests that the threshold α changes continuously with ψ because the corresponding $CRR_n - \alpha$ line keeps moving up or down (see Fig. 5). In this connection, the new notion of α-induced rotation of $CRR_n - \psi$ lines is consistent with the concept built up on the $CRR_n - \alpha$ plane (Yang and Sze 2011). This notion further solidifies the use of the $CRR_n - \psi$ platform as an effective analytical tool in the study of the effect of sustained shear stress on the cyclic strength of sand.

State Dependence of Threshold α

The existence of threshold α has been made conceptually clear on the $CRR_n - \psi$ platform. By using the calibrated $CRR_n - \psi$ trend lines in Fig. 9(a), it is possible to determine a number of threshold α values for Toyoura sand. For example, substituting $CRR_n = \alpha = 0.4$ into the equation of the trend line yields a certain value of ψ. Then, the sand with initial state at this ψ level is expected to have its threshold α at approximately 0.4. The so-obtained threshold $\alpha - \psi$ data points on Toyoura sand are plotted in Fig. 11, together with the experimental threshold α data extracted from Yang and Sze (2011). A striking feature is that a good fit is obtained in regard to the relationship between the threshold α and the state parameter ψ proposed earlier:

$$\alpha_{\text{threshold}} = -2.0854\psi + 0.2205 \quad (6)$$

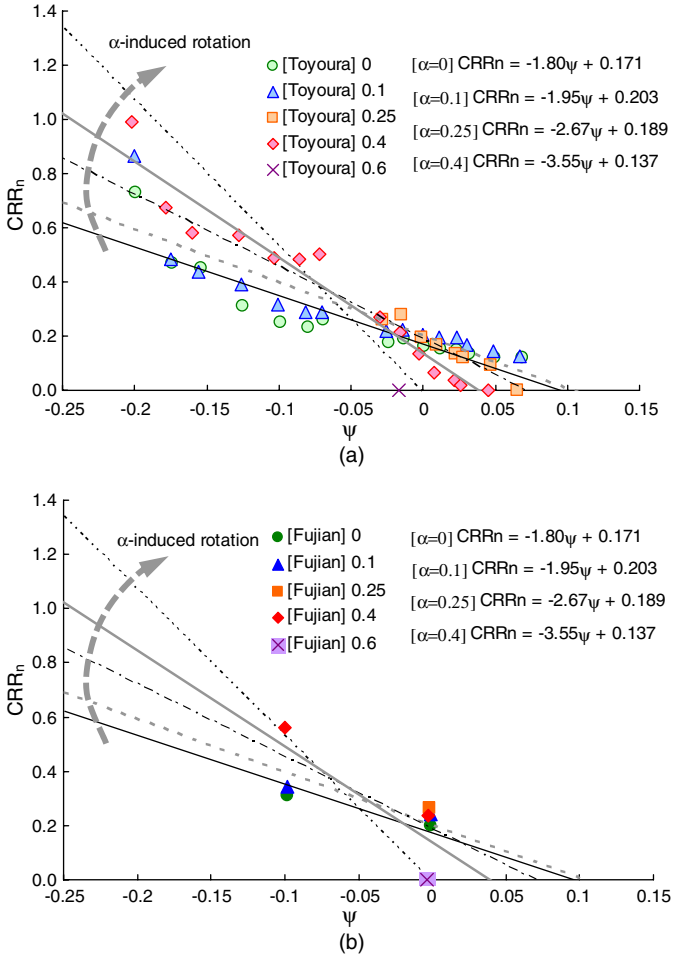

Fig. 9. Correlation between CRR_n and ψ with α value categorization and the concept of α-induced rotation: (a) Toyoura sand; (b) Fujian sand

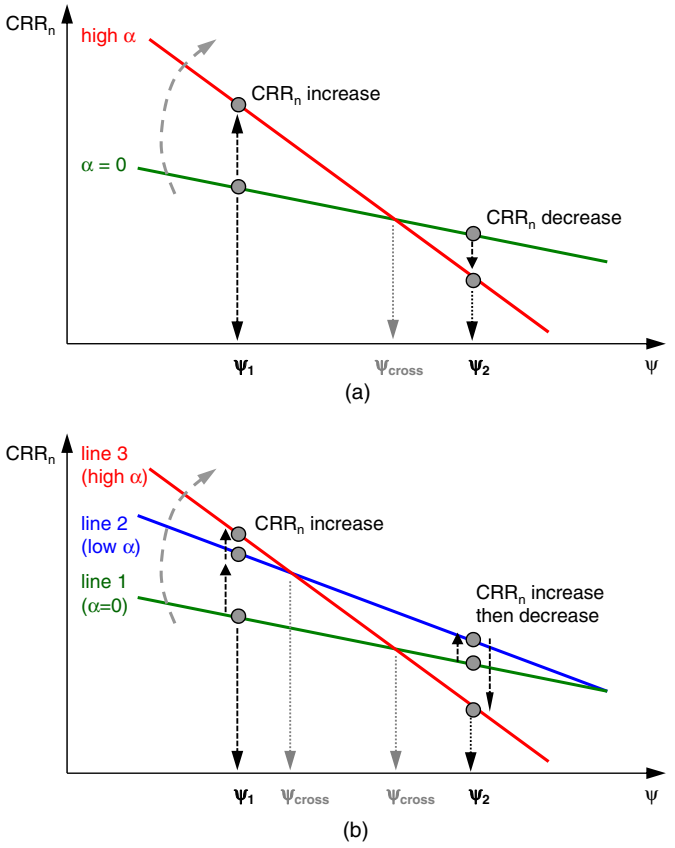

Fig. 10. Tracking of the variations of CRR_n with α at different ψ states: (a) two-line system; (b) three-line system

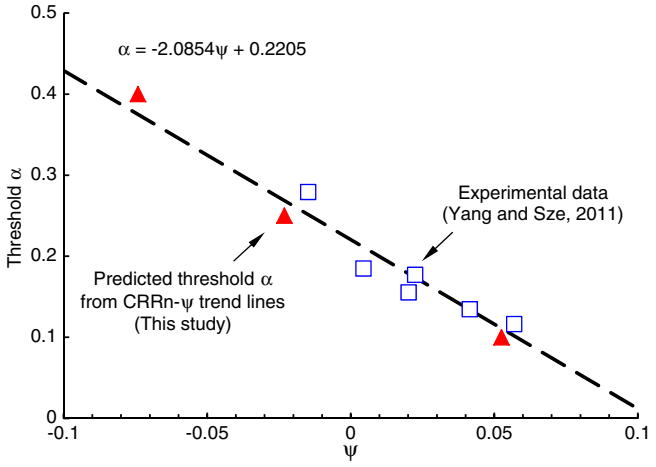

Fig. 11. Threshold α as a function of state parameter

The significance of the preceding equation lies in it allowing straightforward evaluation of the threshold α for a given initial state of sand.

It is of interest to examine whether this relationship works for Fujian sand. In doing so, Fujian sand is considered at the initial state of $D_{rc} = 20\%$ and $p' = 100$ kPa in the $e - \log p'$ plane. Given the critical state line of Fujian sand in Fig. 7, this initial state yields the ψ value of approximately -0.001. Substituting this value into Eq. (6) yields the threshold α of approximately 0.222, which is in good agreement with the experimental result shown in Fig. 5. This example suggests that the form of Eq. (6) has a broader applicability in the evaluation of the threshold α.

Link between Cyclic and Monotonic Loading Paths

Critical Stress Ratio Line

As shown in Fig. 6, the loose sample of Fujian sand, under undrained monotonic loading conditions, exhibits a flow-type behavior characterized by a peak strength at a small strain and then a rapid collapse. Such undrained instability has been discussed by, for example, Lade (1994), Yamamuro and Lade (1997), and Yang (2002). In the $q - p'$ plane, the line passing through the peak point and the origin was referred to as the critical stress ratio (CSR) line by Vaid and Chern (1985), who also attempted to relate the cyclic triaxial behavior of sand to this line. In this study, cyclic loading tests have been performed on truly loose specimens that consistently showed the flow-type failure pattern, and the level of sustained shear stress has been varied over a wide range. It is thus of interest to examine the correspondence between cyclic and monotonic responses under these circumstances.

In doing so, first, the effective stress states at the time when runaway deformation was triggered were measured as the CSR points and plotted in the $q - p'$ plane (Fig. 12). Then, the CSR points determined from monotonic compression and extension tests on the

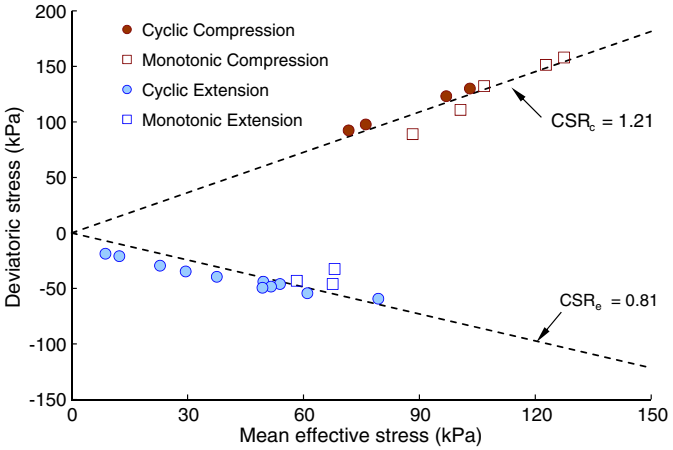

Fig. 12. Critical stress ratio (CSR) lines in compression and extension derived from cyclic and monotonic results

same sand were superimposed on the $q - p'$ plane. Reasonably good agreement is observed between the monotonic and cyclic data. To a first approximation, these data points can be reasonably fit by two straight lines, one on the compression side and one on the extension side. The slope of the CSR line on the compression side is denoted as CSR_c, which is found to have a value of 1.21, giving the mobilized friction angle $\phi_c = 30.2°$. The slope of the CSR line on the extension side, CSR_e, is found to be 0.81, giving the mobilized friction angle $\phi_e = 27.9°$.

To further examine the correspondence between cyclic and monotonic tests, the cyclic loading path of a loose sample of Fujian sand in the absence of sustained shear stress is superimposed by the corresponding monotonic stress path in Fig. 13(a), and the cyclic and monotonic stress paths with the presence of sustained shear stress are compared in Fig. 13(b). In both cases, the initial states for cyclic and monotonic tests were controlled to be the same. Evidently, in the case of zero sustained shear stress, the flow-type deformation in extension attributable to cyclic loading corresponds well with its monotonic counterpart, and this correspondence remains in the case of the presence of sustained shear stress. Although there is some difference in the points at which flow deformation was triggered in the cyclic and monotonic loading conditions, this discrepancy is considered to be the result of the use of stress-controlled loading in cyclic tests but of strain-controlled loading in monotonic tests.

Stress Space View of Cyclic Strength

As discussed previously, the triggering of flow failure or strain softening in sand at loose state is controlled by the compression and extension CSR lines in the stress space. The side on which the flow would be initiated depends on which CSR line is reached first by the cyclic stress path. Fig. 14 illustrates schematically how the presence of a sustained shear stress affects the cyclic strength of sand in the stress space.

If no sustained shear stress is present (i.e., $\alpha = 0$), the initial stress state lies on the p' axis because of the isotropic state and cyclic loading is in complete stress reversal [Fig. 14(a)], meaning that the peak deviatoric stress q_{peak} $(= +q_{cyc})$ is equivalent in magnitude to the valley deviatoric stress q_{valley} $(= -q_{cyc})$. Because the extension CSR line is less steep than the compression CSR line, the distance between the initial state at q_{valley} and the extension CSR line, termed as $\Delta p'_{ext}$, is shorter than that between the state at q_{peak} and the compression CSR line, termed as $\Delta p'_{comp}$. When the effective stress path moves toward the two lines as a result of progressive

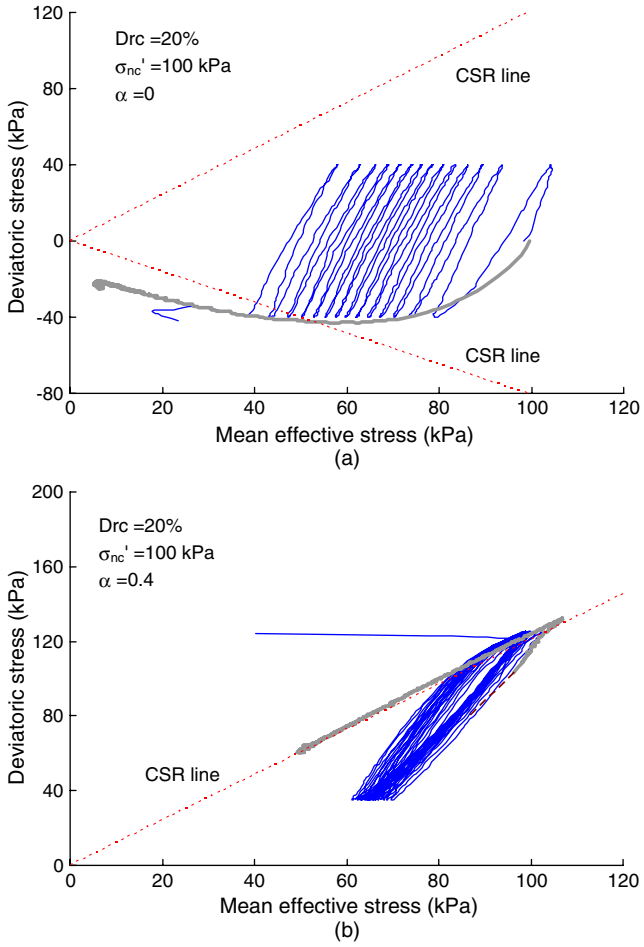

Fig. 13. Correspondence between monotonic and cyclic stress paths at loose state: (a) without sustained shear stress; (b) with sustained shear stress

buildup of pore water pressure, it will eventually reach the extension CSR line first. This explains why flow deformation was always triggered in extension in the case of zero sustained shear stress.

When a sustained shear stress is present at a low level, say $\alpha = 0.1$, the addition of q_s will take the initial stress state to somewhere above the p' axis [Fig. 14(b)]. If the same distance of stress path migration is assumed to be required to cause failure in the same number of cycles as the case of $\alpha = 0$, then q_{cyc} needs to be increased such that q_{valley} $(= q_s - q_{cyc})$ can maintain the previous $\Delta p'_{ext}$. In this case, although q_{peak} $(= q_s + q_{cyc})$ is also increased and the corresponding state becomes closer to the compression CSR line, the resulting $\Delta p'_{comp}$ may still be greater than $\Delta p'_{ext}$. This explains why the presence of sustained shear stress at a low level with part stress reversals leads to an increase in cyclic strength, and the strength tends to increase continuously with α as long as q_s does not rise to a too high level (i.e., $\Delta p'_{comp}$ remains greater than $\Delta p'_{ext}$). Under such circumstances, failure will always be triggered in extension.

If the sustained shear stress is present at a high level, say $\alpha = 0.4$, q_s will become quite large such that the initial stress state is closer to the compression CSR line [Fig. 14(c)]. As a result, a small q_{cyc} is sufficient to bring the state at q_{peak} to a position such that $\Delta p'_{comp}$ is smaller than $\Delta p'_{ext}$. This means the sample will fail in compression, not in extension. In this case, q_{cyc} becomes smaller than q_s such that q_{valley} is in compression and stress reversal is

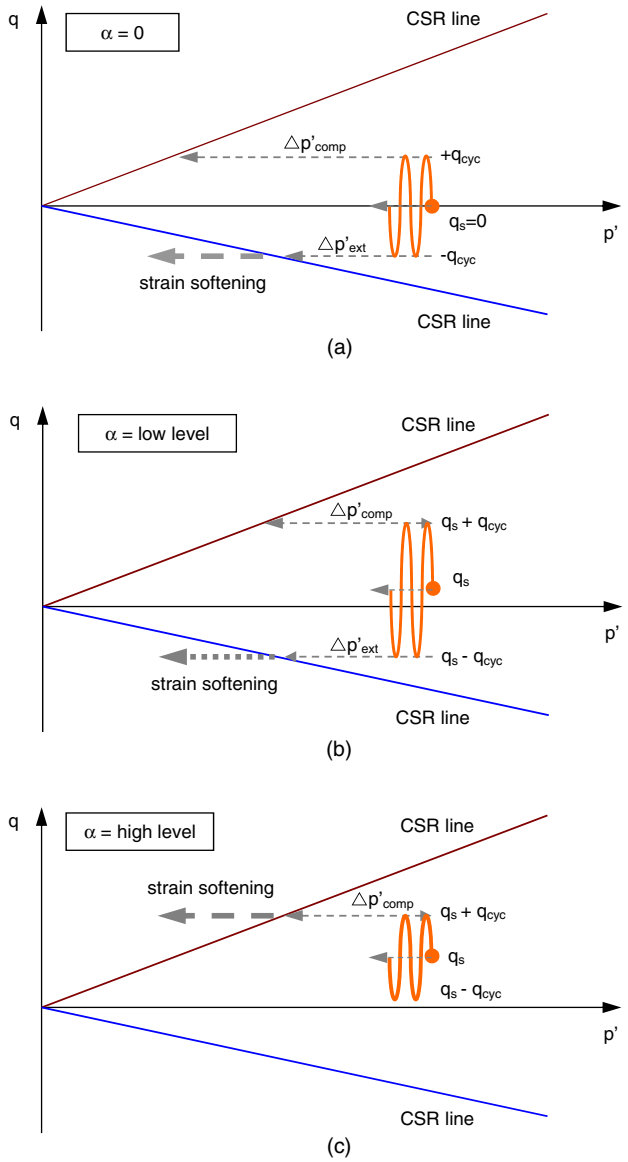

Fig. 14. Stress space view connecting CSR lines with cyclic stress path: (a) zero α; (b) low α value; (c) high α value

absent. A further increase in α will certainly bring the initial stress state even closer to the compression CSR line. This is why the cyclic strength keeps reducing at high α levels and this behavior is always associated with the case of no stress reversal.

The previous illustrations and explanations, although qualitative, provide a rational framework in understanding the effect of sustained shear stress on the cyclic behavior and strength of sand.

Summary and Conclusions

This paper presents experimental results from a series of cyclic tests on Fujian sand under various levels of sustained shear stress and compares these results with earlier results on Toyoura sand. Selected results from a series of monotonic tests on Fujian sand are also presented to develop a better interpretation in the framework of critical state soil mechanics. The major points of the study can be summarized as follows:

- Moist tamped specimens of Fujian sand, like Toyoura sand, exhibit exclusively three failure patterns when subjected to cyclic loading under sustained shear stress. Sudden flow-type failure is the unique mode of loose specimens, irrespective of the presence or absence of sustained shear stress. Specimens at medium dense state experience cyclic mobility whenever the degree of stress reversal is not minimal; if stress reversal is absent, the mode of plastic strain accumulation then becomes dominant.
- For the range of initial states tested, the presence of sustained shear stress always enhances the cyclic strength of sand at medium dense state. Loose sand, however, shows an initial increase and then a decrease in strength with an increasing level of sustained shear stress. The use of a no-stress-reversal line to predict the threshold α is confirmed to be effective for Fujian sand as well.
- The CRR_n values of Fujian sand correlate well with the state parameter ψ. The new data fit well with the relationship previously established on Toyoura sand. The use of ψ is able to take into account the difference in physical properties of the sand types tested and meanwhile to consider the influence of both density and confining stress in a collective manner.
- The threshold α of loose Fujian sand can be predicted by the linear relationship previously proposed between the threshold α and ψ by using data for Toyoura sand, suggesting that this relationship has a potential for broader application.
- On the $\mathrm{CRR}_n - \psi$ platform, it has been found that increasing the α level leads to clockwise rotation of the $\mathrm{CRR}_n - \psi$ trend line. This means that the rate of strength reduction attributable to increasing contractiveness is always enhanced under greater α levels. The threshold α at a certain ψ state is the α level for which the $\mathrm{CRR}_n - \psi$ line positions the upmost among others at this ψ. This new finding offers a consistent view of the $\mathrm{CRR}_n - \alpha$ response.
- The compression and extension CSR lines of Fujian sand can be consistently established in the stress space from both cyclic and monotonic loading tests. With the aid of the distances between the initial stress states and the two CSR lines, questions as to when and in what direction the flow failure will take place upon undrained cyclic shearing can be explained rationally.

Acknowledgments

The work reported in this paper was supported by the Research Grants Council of Hong Kong under Grant No. 719105. This support is gratefully acknowledged. The financial support provided by the University of Hong Kong through the Outstanding Young Researcher Award scheme is also highly acknowledged.

References

Been, K., and Jefferies, M. (1985). "A state parameter for sands." *Géotechnique*, 35(2), 99–112.

Boulanger, R. W. (2003). "Relating K_α to relative state parameter index." *J. Geotech. Geoenviron. Eng.*, 129(8), 770–773.

Harder, L. F. Jr., and Boulanger, R. W. (1997). "Application of K_σ and K_α correction factors." *Proc., NCEER Workshop on Evaluation of Liquefaction Resistance of Soils*, National Center for Earthquake Engng. Res., State Univ. of New York at Buffalo, Buffalo, NY, 167–190.

Hyodo, M., Tanimizu, H., Yasufuku, N., and Murata, H. (1994). "Undrained cyclic and monotonic triaxial behavior of saturated loose sand." *Soils Found.*, 34(1), 19–32.

Idriss, I. M., and Boulanger, R. W. (2003). "Estimating $K\alpha$ for use in evaluating cyclic resistance of sloping ground." *Proc., 8th U.S.-Japan Workshop on Earthquake Resistance Design of Lifeline Facilities and Countermeasures against Liquefaction*, *Rep. MCEER-03-0003*, 449–468.

Idriss, I. M., and Boulanger, R. W. (2008). "Soil liquefaction during earthquakes." *EERI MNO-12*, Earthquake Engineering Research Institute, Oakland, CA.
Ishihara, K. (1996). *Soil behaviour in earthquake geotechnics*, Clarendon Press, Oxford.
Jefferies, M., and Been, K. (2006). *Soil liquefaction: a critical state approach*, Taylor & Francis, London.
Lade, P. V. (1994). "Instability and liquefaction of granular materials." *Comput. Geotech.*, 16(2), 123–151.
Mohamad, R., and Dobry, R. (1986). "Undrained monotonic and cyclic strength of sand." *J. Geotech. Eng.*, 112(10), 941–958.
Schofield, A. N., and Wroth, C. P. (1968). *Critical state soil mechanics*, McGraw-Hill, London.
Seed, H. B. (1979). "Soil liquefaction and cyclic mobility evaluation for level ground during earthquakes." *J. Geotech. Engrg. Div.*, 105(GT2), 201–255.
Seed, H. B. (1983). "Earthquake-resistant design of earth dams." *Proc., Symp. Seismic Des. Earth Dams and Caverns*, ASCE, New York, 41–64.
Seed, H. B., and Lee, K. L. (1966). "Liquefaction of saturated sands during cyclic loading." *J. Soil Mech. Found. Div.*, 92(SM6), 105–134.
Seed, R. B., and Harder, L. F. Jr (1990). "SPT-based analysis of cyclic pore pressure generation and undrained residual strength." *Proc., H. Bolton Seed Memorial Symp.*, BiTech Publishers Ltd., Vancouver, 351–376.
Toki, S., Tatsuoka, F., Miura, S., Yoshimi, Y., Yasuda, S., and Makihara, Y. (1986). "Cyclic undrained triaxial strength of sand by a cooperative test program." *Soils Found.*, 26(3), 117–128.
Vaid, Y. P., and Chern, J. C. (1985). "Cyclic and monotonic undrained response of sands." *Advances in the art of testing soils under cyclic loading conditions*, ASCE, Reston, VA, 171–176.
Vaid, Y. P., Stedman, J. D., and Sivathayalan, S. (2001). "Confining stress and static shear effects in cyclic liquefaction." *Can. Geotech. J.*, 38(3), 580–591.
Verdugo, R., and Ishihara, K. (1996). "The steady state of sandy soils." *Soils Found.*, 36(2), 81–91.
Yamamuro, J. A., and Lade, P. V. (1997). "Static liquefaction of very loose sands." *Can. Geotech. J.*, 34(6), 905–917.
Yang, J. (2002). "Non-uniqueness of flow liquefaction line for loose sand." *Géotechnique*, 52(10), 757–760.
Yang, J., Savidis, S., and Roemer, M. (2004). "Evaluating liquefaction strength of partially saturated sand." *J. Geotech. Geoenviron. Eng.*, 130(9), 975–979.
Yang, J., and Sze, H. Y. (2011). "Cyclic behaviour and resistance of saturated sand under non-symmetrical loading conditions." *Gèotechnique*, 61(1), 59–73.
Youd, T. L., et al. (2001). "Liquefaction resistance of soils: summary report from the 1996 NCEER and 1998 NCEER/NSF workshops on evaluation of liquefaction resistance of soils." *J. Geotech. Geoenviron. Eng.*, 127(10), 817–833.